



**HAL**  
open science

# Stochastic Linear Quadratic Optimal Control of Speed and Position of Multiple Trains on a Single-Track Line

Chiara Bersani, Matteo Cardano, Stefano Lavaggi, Roberto Sacile, Simona Sacone, Mohamed Sallak, Enrico Zero

## ► To cite this version:

Chiara Bersani, Matteo Cardano, Stefano Lavaggi, Roberto Sacile, Simona Sacone, et al.. Stochastic Linear Quadratic Optimal Control of Speed and Position of Multiple Trains on a Single-Track Line. IEEE Transactions on Intelligent Transportation Systems, 2023, 24 (9), pp.9110 - 9120. 10.1109/TITS.2023.3268319 . hal-04119979

**HAL Id: hal-04119979**

**<https://hal.science/hal-04119979>**

Submitted on 6 Dec 2023

**HAL** is a multi-disciplinary open access archive for the deposit and dissemination of scientific research documents, whether they are published or not. The documents may come from teaching and research institutions in France or abroad, or from public or private research centers.

L'archive ouverte pluridisciplinaire **HAL**, est destinée au dépôt et à la diffusion de documents scientifiques de niveau recherche, publiés ou non, émanant des établissements d'enseignement et de recherche français ou étrangers, des laboratoires publics ou privés.

# Stochastic Linear Quadratic Optimal Control of Speed and Position of Multiple Trains on a Single-Track Line

Chiara Bersani<sup>1</sup>, Matteo Cardano, Stefano Lavaggi, Roberto Sacile<sup>2</sup>, *Member, IEEE*,  
 Simona Sacone, *Member, IEEE*, Mohamed Sallak, and Enrico Zero<sup>3</sup>, *Member, IEEE*

**Abstract**—In the European Rail Traffic Management System (ERTMS), the Route Control Centre System (RCCS) supervises the distance between consecutive trains and generates movement authorities, i.e. the permission for a train to move to a specific location within the constraints of the infrastructure and with supervision of speed. In this work, a control model aimed at determining the speed and position of a train platoon within a sector of the rail network is presented. The central controller, i.e. the RCCS, receives information about the current position and speed of trains and it sends them decisions about optimal corrective actions for each train. Priorities of trains are handled to respect the planned timetable, taking into account the train dynamics, limitations in divergences of positions, speeds, and tractive effort, as well as minimum distances between consecutive trains. The control approach is based on a quite innovative linear quadratic regulator allowing the definition of stochastic constraints. The validation of the model is based on data collected from a RCCS for a section of the high-speed Paris-London line.

**Index Terms**—ERTMS, RCCS, stochastic linear quadratic control, train scheduling, train platooning.

## I. INTRODUCTION

THE European Rail Traffic Management System (ERTMS) legislation covers two main aspects: its technical specifications and the process for putting the system into service. The Technical Specifications of Interoperability for Control Command and Signaling (TSI CCS) is an essential document describing the ERTMS. The revised TSI for the onboard and trackside CCS subsystems were adopted by the European Commission Regulation (EU) 2016/919 published in the Official Journal of the European Union on 15th June 2016 [1]. The Interoperability Directive (2008/57/EC) defines several essential requirements to be met for interoperability, which include safety, reliability and availability, health, environmental protection, and technical compatibility along with others specific to certain subsystems [2]. The ERTMS application

Manuscript received 2 September 2021; revised 23 February 2022, 30 May 2022, 3 October 2022, and 9 March 2023; accepted 10 April 2023. Date of publication 28 April 2023; date of current version 30 August 2023. The Associate Editor for this article was S. E. Li. (*Corresponding author: Enrico Zero.*)

Chiara Bersani, Matteo Cardano, Stefano Lavaggi, Roberto Sacile, Simona Sacone, and Enrico Zero are with the Department of Informatics, Bioengineering, Robotics, and Systems Engineering, University of Genoa, 16126 Genoa, Italy (e-mail: enrico.zero@dibris.unige.it).

Mohamed Sallak is with Laboratoire Heudiasyc-UMR CNRS 7253, Université de Technologie de Compiègne, 60200 Compiègne, France.

Digital Object Identifier 10.1109/TITS.2023.3268319

includes three different levels [3]. While ERTMS levels 1 and 2 are in operation on several railway lines, ERTMS Level 3 represents an important innovation, and it is currently under test. ERTMS Level 3 has significant advantages for railway engineers, since it eliminates some trackside equipment, and it introduces the moving block signaling approach. In moving block signaling, trains are given permission to move to a specific position anywhere on the track. A safe ‘envelope’ of empty track moving with each train is generated in real time. This envelope can be sized according to the braking performance and the speed of that specific train (e.g., low-speed train closer together, and high-speed trains further apart). This is in contrast with the traditional fixed block signaling in which trains are granted permission to move to a pre-defined, fixed position.

The main difference with respect to ERTMS Level 2 is that the train autonomously detects train integrity, rather than requiring the track circuit to perform this task. So, in ERTMS Level 3, the Radio Block Centre (RBC) determines the train location in co-operation with the onboard Train Integrity Monitoring (TIM) System. Train detection equipment can therefore be removed from the track, and the train separation distance is based on these moving block sections. In this way, the RCCS can fluidly monitor distances between trains, and the headway between trains is significantly reduced.

In brief, ERTMS Level 3 operates as follows:

- the onboard computer determines the train position and verifies that the current speed corresponds to the travelled distance;
- the train sends its position to the control center via radio signals;
- the control center receives all trains position and sends the new movement authorities (MAs) to each train;
- the onboard computer calculates the speed profile and the braking points and displays them to the train driver.

The moving block is defined as an automated control system allowing each train to receive a movement authority info from the control center. The control center has to have a continuous dialogue with all the trains to know their speed and position. Similarly a Communications-Based Train Control (CBTC) is a railway signaling system that makes use of the telecommunications between the train and track equipment for

the traffic management and infrastructure control [4], [5]. The CBTC is based on the principle that trains determine their positions themselves and transmit it to wayside equipment. CBTC assures that the space between trains is always safe. However, CBTC is not always interoperable with other suppliers' products. This issue is a major problem for large-scale mainline networks that use many interoperating products. ERTMS Level 3 is then an alternative solution. Moreover, ERTMS Level 3 enable the adoption of moving block, which means that two trains in succession can run at lower speeds. In ERTMS level 3, the train location and train integrity supervision are performed by the trackside RBC in cooperation with the train which sends position reports and train integrity information to RBC. The track to train communication is bidirectional and based on Euroradio whereas Eurobalises are mainly used as spot transmission devices for location referencing (position reports) [6]. The MAs (i.e., permission for a train to move to a specific location with supervision of speed) are generated trackside and are transmitted to the train via Euroradio (GSM-R). These MAs are displayed on a Driver Machine Interface (DMI) installed in the driver's cab. The driver shall observe the displayed information on the DMI and shall react as required by the operational rules. More specifically, MA gives the maximum speed at which a train is allowed to reach the end of its Avement Authority. Trackside equipment knows each ERTMS controlled train individually by using the ERTMS identity of the leading ERTMS on board equipment. These informations are then updated according to the track situations and movement authority is renewed. So, ERTMS Level 3 provides a continuous speed supervision system, which also protects against overrun of the authority.

In this paper, we propose a centralized control approach in which all the trains within a particular sector of a single track-line send information about their position and speed to the local RCCS. With reference to the recent review paper [7] on dynamic scheduling, operation control and their integration in high-speed railways, this approach can be classified as operation control of high-speed trains, specifically cooperative control of multiple trains. In our approach, multiple trains are present in the same sector, and they are jointly regulated. Specifically, the RCCS can compute and forward the optimal corrective decisions to each train. In this context, the RCCS objective is to issue control instructions, with different levels of train priority, to bring actual positions closer to scheduled positions, considering the train dynamics, limitations in divergences of positions, speeds, and tractive effort, as well as the headway between consecutive trains in the platoon. It must be noted that in the proposed approach the size of the platoon in a given sector, that is, the number of trains, can vary during time. From a control viewpoint, the main novelty is the adoption of a quite recent control methodology [8] which allows to limit the expected quadratic divergence of the variables related to positions, speeds, and tractive effort for each train. According to the state of the art, the set of multiple trains is hereinafter defined as a train platoon [9] following a safe train distance strategy not focusing on the two-train tracking, but on the whole efficiency of the train platoon. It is worthwhile to underline that as the scheduled

headway in high-speed trains is in the order of some minutes, the expected minimum safe distance between two consecutive trains is of several kilometres.

## II. STATE OF THE ART

In [10], the authors proposed a relationship between probabilities of emergency train braking as a function of distance between subsequent trains. They considered the following main parameters: train speed, emergency braking distance, train length, position localization error. They studied a scenario with two successive trains using the same track. The first train automatically checks its integrity and determines its position. Next, the resulting status message is sent through the GSM-R module to the nearest RBC [11]. Transmission errors mean that there is a particular probability value for the message being lost. The likelihood of successful transmission is assumed to follow an exponential distribution. Finally, they compute the probability of a train successfully being stopped by emergency braking as a function of distance between trains, using results obtained from a simulation. In [12], the authors developed models and algorithms for real-time conflict resolution adapted for both fixed block (ERTMS Level 2) and moving block (ERTMS Level 3) signaling safety concepts. The train timetables are currently implemented taking into account possible delays due to disturbances when travelling. In [13], the authors proposed a robust model predictive control (MPC) for train regulation in underground railway transportation. In [14], a decentralized MPC has been developed to manage the position of one train and the headway between two consecutive vehicles by the assumption to receive data related to distance, speed, and brake demand from the preceding train. Also, the speed curve optimization, where the controller must track the optimal speed profile to assure safe and effective operations appear relevant in the tracking control of rail trains. In [15], an optimization model based on a genetic algorithm is presented for the optimal speed curve seeking. Several issues still remain open before the ERTMS Level 3 can become operational. Primarily, the train integrity issue relating to the use of additional complex equipment in the train has to be addressed. To handle situations such as failures of onboard equipment, some redundancy architectures need to be proposed and their dependability parameters (Mean Time To Failure MTTF, availability, etc.) quantified. Then, the safety standard must clearly explain all the design steps and the required dependability parameters for each additional subsystem in the switch from Level 2 to Level 3. In [16], the authors applied a robust team decision theory to control noncritical train distances in moving blocks, such as in ERTMS Level 3. Also, in [17], the authors aimed at scheduling a set of trains from opposite sides along a single track which consisted in intermediate stations. The trains could pass each other at those stations while traversal times of the trains on the blocks between the stations only depended on the block lengths but not on the trains. In [18], the authors proposed a decision-making framework to support a critical decision process by developing a SWOT (strengths, weaknesses, opportunities, and threats) analysis based on external and internal factors that simultaneously enhance and constrain the ERTMS implementation.



Fig. 1. A platoon of  $M$  trains on a single-track line. Trains are travelling from left to right and are identified by the numbers  $1, \dots, M$ , ascending according to their schedule.

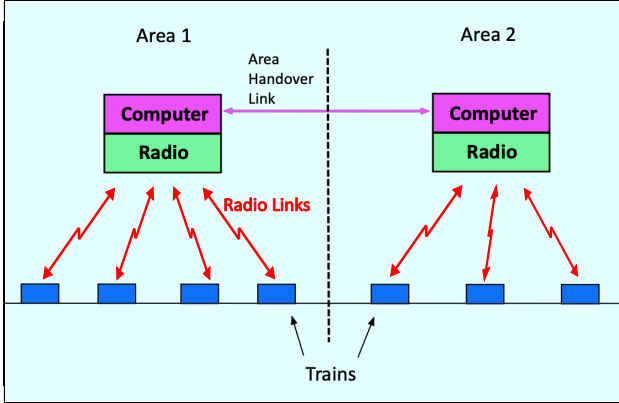


Fig. 2. Transmission data when using moving blocks.

In this paper, we propose an approach that could be used in RCCS's to control speeds among trains on a single-track line, under safe situations, that is when moving blocks are however securely separated. A centralized stochastic optimal control model has been developed considering train's position, speed, and related tractive force. Section III describes the proposed approach.

### III. MODEL FORMULATION

Consider a platoon of  $M$  trains travelling on a single-track line in a sector of the rail network. The position of each train in the platoon is identified by a number. The first train in the platoon is identified with number 1, the second one with 2, and the last one with  $M$  (Fig. 1).

#### A. Information Model

The reference information model is the one proposed for ERTMS Level 3. A communication network allows information exchange among the trains themselves and with an information center, i.e. the RCCS, responsible for one sector (Fig. 2). In the case of a single track, each train can transmit information, e.g. its current GPS position and speed, to the center.

Transmission delays and the time required to compute the optimal control law defining the train tractive effort are assumed to be negligible. This assumption obviously implies an efficient communication channel and a fast, efficient control algorithm.

At the operational decisional level, the train movements are represented by the classical time distance graphs which visualize the position of trains in space and time according to constant speed values. The associated train tractive effort in steady state conditions with no acceleration may be computed by the model introduced in the following subsection.

#### B. Model of the Train Motion

A recent exhaustive description of the train motion equations can be found in [19]. The general equation for the motion of the  $i$ -th train, known as Lomonosoff's equation, can be written as follows:

$$\begin{cases} \frac{dx_{i,1}(t)}{dt} = x_{i,2}(t) \\ W_i \frac{d^2x_{i,2}(t)}{dt^2} = f_i(t) - (C_i^a + C_i^b x_{i,2}(t) + C_i^c x_{i,2}^2(t)) \\ -W_i g \sin \alpha_i(t) \quad i = 1 \dots M \end{cases} \quad (1)$$

where:

- $x_{i,1}(t)[m]$  and  $x_{i,2}(t)[m/s]$  are respectively the position and the speed of the  $i$ -th train at time  $t$ ;
- $f_i(t)[kN]$  is the tractive effort at time  $t$ ;
- $C_i^a, C_i^b, C_i^c$  are the Davis constants related to resistance, where:
  - $C_i^a[kN]$  corresponds to mechanical resistance;
  - $C_i^b[\frac{kN}{m/s}]$  corresponds to viscous mechanical resistance;
  - $C_i^c[\frac{kN}{m^2/s}]$  corresponds to aerodynamic resistance;
- $W_i[tonnes]$  is the effective mass including rotary allowance;
- $W_i[tonnes]$  is the train mass;
- $\alpha_i(t)[\cdot]$  is the slope angle of the position of the  $i$ -th train at time  $t$ .

#### C. Reference Trajectory

A timetable graph is usually represented by a time/position graph. It can be defined by the planned position  $\bar{x}_{i,1}(t)$  at each time  $t$ , and, consequently, the desired average speed  $\bar{x}_{i,2}(t)$ , which is defined as constant in each time interval. A reference trajectory, as described by a timetable graph, is so planned as a list of desired positions in a given planning interval  $[t_p, t_{p+1})$ . The desired position is described by the progressive distance related to the specific track. For the  $i$ -th train, the planned information is given by a list of planned values. In Fig. 3, an example of timetable graph and related notation are represented for two trains 1 and 2. Specifically,  $t_p$  is the time in which a train is planned to be in a given position, for example entering a railway section. Each interval  $[t_p, t_{p+1})$  is also further discretized into  $N_p$  time intervals indexed with  $k$  and having the same duration equal to  $\Delta t_p = \frac{(t_{p+1}-t_p)}{N_p}$ .

#### D. Linearization of the Motion Model

Equation (1) is nonlinear, due to a quadratic term function of the speed. A linear approximation is introduced, centered around a working state/control couple  $(\bar{x}_{i,2}, \bar{f}_i)$  in steady condition with acceleration equal to zero, where  $\bar{f}_i$  is given by

$$\bar{f}_i = (C_i^a + C_i^b \bar{x}_{i,2} + C_i^c \bar{x}_{i,2}^2) + W_i g \sin \alpha_i \quad (2)$$

At instant  $t_p$  the planned position and speed of the  $i$ -th train are  $\bar{x}_{i,1}(t_p)$  and  $\bar{x}_{i,2}(t_p)$ , corresponding to the tractive

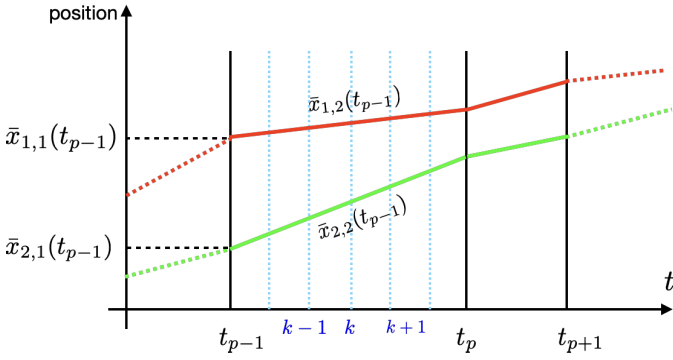


Fig. 3. Position of two trains, i.e.  $i = 1..2$ , in a planned train graph. In each time interval,  $[t_p, t_{p+1})$  the speed is constant.

effort  $\bar{f}_i(t_p)$ . The system can be linearized for each planned instant  $\bar{t}_p$  around the state vector given by:

$$\bar{x}_{i,p} = [\bar{x}_{i,1}(t_p) \ \bar{x}_{i,2}(t_p)]' \quad (3)$$

At any instant  $t \in [t_p, t_{p+1})$  let  $\delta x_{i,p}(t)$  and  $\delta f_{i,p}(t)$  be the variations around such state and control given by:

$$\delta x_{i,p}(t) = [x_{i,1}(t) - \bar{x}_{i,1}(t_p) \ x_{i,2}(t) - \bar{x}_{i,2}(t_p)]' \quad (4)$$

$$\delta f_{i,p}(t) = f_i(t) - \bar{f}_i(t_p) \quad (5)$$

The resulting linearized equation in matrix formulation is:

$$\frac{d\delta x_{i,p}(t)}{dt} = A_p \delta x_{i,p}(t) + B \delta f_{i,p}(t) + \underline{w}_\alpha(t) + \underline{w}_p(t) \quad (6)$$

where

$$A_p = \begin{bmatrix} 0 & 1 \\ 0 & -\frac{(C_i^b + 2C_i^c \bar{x}_{i,2}(t_p))}{W_i'} \end{bmatrix} \quad (7)$$

$$B = \begin{bmatrix} 0 \\ \frac{1}{W_i'} \end{bmatrix} \quad (8)$$

and

$$\underline{w}_\alpha(t) = \begin{bmatrix} 0 \\ -\frac{W_i}{W_i'} g \sin \alpha_i(t) \end{bmatrix} \quad (9)$$

and  $\underline{w}_p(t)$  is a noise given to imperfections of the model as well as by other technical and environmental components. The model given by (4)-(9) can be so discretized according to the zero-order hold method. The matrices related to the discretized model are indicated as  $\bar{A}_p$  and  $\bar{B}$ .

$$\delta x_{i,p}(k+1) = \bar{A}_p \delta x_{i,p}(k) + \bar{B} \delta f_{i,p}(k) + \underline{w}_{\alpha,p}(k) + \underline{w}_p(k) \quad (10)$$

$$k = 0, \dots, N_p - 1$$

assuming that  $k = 0$  corresponds to  $t = t_p$  and a generic value of  $k$  indicates  $t = t_p + k * \Delta t_p$ . In addition, there are physical constraints that should be introduced with respect to this model, such as the maximum values which the physical variables as speed, acceleration, and force may assume. One specific constraint, which is often given as a characteristic of the specific train, limits the tractive effort to a maximum value which is almost constant at low speeds, while at higher speeds it is inversely proportional to the speed and directly proportional to the train power. This is respectively due to the

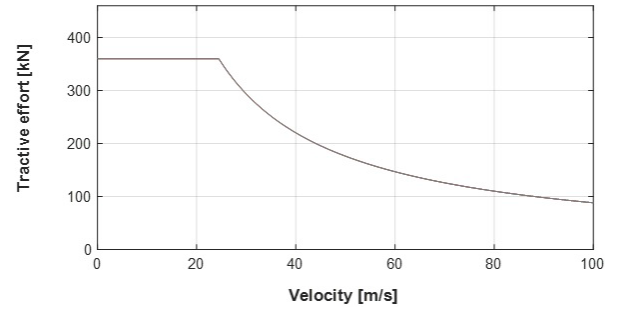


Fig. 4. Tractive effort vs speed in high-speed trains.

adherence of the tractive effort and to the power limit. This constraint is qualitatively shown for a generic high-speed train in Fig. 4.

### E. Control Model

A control model is proposed to provide the train driver with values of the tractive force to track a desired trajectory in time and space as required by the RCCS. Specifically, the goal of the control model is to keep the state of each train, in terms of desired position and speed, around the planned value. This objective can be achieved by minimizing the quadratic deviation of the state from the desired values. In addition, for safety reasons, the control must also assure that the expected headways between consecutive trains do not vary above a given value.

Without no loss of generalization and for sake of simplicity, hereinafter, it is supposed that the track has no slope, that is (9) is a zero vector.

Based on this model formulation, the control problem hereinafter quoted as  $\mathcal{P}_p$  defined on time interval  $[t_p, t_{p+1})$ , can be expressed as:

$$J^* = \min_{\delta f_{i,p}(k), k=0, \dots, N_p-1} \sum_{i=1}^M \sum_{k=1}^{N_p} \mathbf{E}[\delta x_{i,p}'(k) Q \delta x_{i,p}(k)] + \sum_{i=1}^M \sum_{k=0}^{N_p-1} \mathbf{E}[\delta f_{i,p}'(k) R \delta f_{i,p}(k)] \quad (11)$$

s.t. (6) and

$$\mathbf{E}[\delta x_{i,p}'(k) \delta x_{i,p}(k)] \leq \underline{x}_{i,p}^{\text{MAX}}(k) \quad (12)$$

$$i = 1, \dots, M \quad k = 1, \dots, N_p$$

$$\mathbf{E}[\delta f_{i,p}^2(k)] \leq \underline{f}_{i,p}^{\text{MAX}}(k) \quad (13)$$

$$i = 1, \dots, M \quad k = 0, \dots, N_p - 1$$

$$\mathbf{E}[(\delta x_{i-1,p}(1, k) - \delta x_{i,p}(1, k))^2] \leq \underline{d}_{i,p}^{\text{MAX}}(k) \quad (14)$$

$$i = 2, \dots, M \quad k = 1, \dots, N_p$$

For each train, the objective function (11) minimizes the quadratic divergence, related to the real and planned positions, speeds, and tractive efforts.

Constraints (12), (13), (14), defined as power constraints, limit the variance of the state and of the control within a certain interval specific to each train and for each time instant or interval.



It should be noted that in each time interval  $t \in [t_p, t_{p+1})$ , each planned train position varies between  $\bar{x}_{i,1}(t_p)$  and  $\bar{x}_{i,2}(t_{p+1})$ , while the speed is constant, that is  $\bar{x}_{i,1}(t_p^+) = \bar{x}_{i,1}(t) = \bar{x}_{i,1}(t_{p+1}^-)$ ,  $\forall t \in [t_p, t_{p+1})$ . As a consequence, the reference acceleration is always zero.

So, for the position element  $x_{i,1}(k)$ ,  $k = 0, 1, \dots, N_p$ , this is not completely adherent with what required by the cost function (11). This problem can be faced at least according to three possible strategies. The first strategy is to modify the cost function considering the deviation from the planned position at each instant  $k = 0, 1, \dots, N_p$ , transforming the problem in a tracking problem. In addition, the constraints (12) should also take into account the squared value of desired position in the first component of the vector on the right hand side  $\underline{x}^{\max_{i,p}}$ .

A second option could be to penalize with a very weak cost the position deviation in the diagonal elements of matrix  $Q$ , but, as above, modifying properly the constraints (12).

A third option could be to define a new reference system, where, at each instant  $k = 0, 1, \dots, N_p$ , each position is  $x_{i,1}(k)$  is referred to a desired planned position  $\bar{x}_{i,1}(k)$  and not to  $\bar{x}_{i,1}(t_p)$ . This option implies some additional transformation which is omitted here for sake of readability. This third option has been chosen in the case study.

Constraint (14) requires that the difference between the divergence of the positions (with respect to the planned ones) of two consecutive trains  $i-1$  and  $i$  must be limited by  $d_{i,p}^{\max}(k)$ , which is the maximum expected quadratic deviation of the safe distance.

#### F. Adding Smoothness Penalty

To reduce sudden variations of the resulting tractive force in  $P^N$ , an additional penalty on the control smoothness has been introduced by minimizing the square of the difference  $\delta f_{i,p}(k) - \delta f_{i,p}(k-1)$ . To implement the smoothing penalty, the problem has been modified by augmenting the state with  $\delta f_{i,p}(k)$ , as shown below. Let us define:

$$\begin{aligned} \delta \delta f_{i,p}(k) &= \delta f_{i,p}(k) - \delta f_{i,p}(k-1) \quad i = 1, \dots, M \\ & \quad k = 0, \dots, N_p - 1 \end{aligned} \quad (15)$$

with

$$\delta f_{i,p}(-1) = \delta f_{i,p-1}(N_{p-1}) \quad (16)$$

where  $\delta f_{i,p-1}(N_{p-1})$  is the value of  $\delta f_{i,p-1}$  at the end of the previously linearized time interval, if available, 0 otherwise.

The equation (10) can be so rewritten as:

$$\begin{aligned} \begin{bmatrix} \delta x_{i,p}(k+1) \\ \delta f_{i,p}(k) \end{bmatrix} &= \begin{bmatrix} \bar{A}_p & \bar{B} \\ 0 & 1 \end{bmatrix} \begin{bmatrix} \delta x_{i,p}(k) \\ \delta f_{i,p}(k-1) \end{bmatrix} \\ &+ \begin{bmatrix} \bar{B} \\ 1 \end{bmatrix} \delta \delta f_{i,p}(k) + \begin{bmatrix} \underline{w}_p(k) \\ 0 \end{bmatrix} \end{aligned} \quad (17)$$

Thus, for the  $i$ -th train, we can consider to rewrite (10) as

$$\delta \bar{x}_{i,p}(k+1) = \bar{A}_p \delta \bar{x}_{i,p}(k) + \bar{B} \delta \delta f_{i,p}(k) + \bar{W}_p(k) \quad (18)$$

where

$$\begin{aligned} \delta \bar{x}_{i,p}(k+1) &= \begin{bmatrix} \delta x_{i,p} \\ \delta f_{i,p}(k-1) \end{bmatrix} \\ \bar{A}_p &= \begin{bmatrix} \bar{A}_p & \bar{B} \\ 0 & 1 \end{bmatrix} \quad \bar{B} = \begin{bmatrix} \bar{B} \\ 1 \end{bmatrix} \quad \bar{W}_p(k) = \begin{bmatrix} \underline{w}_p(k) \\ 0 \end{bmatrix} \end{aligned}$$

In problem  $\mathcal{P}_p$ , the cost function (11) can be consequently modified and for a more compact notation can be written in matrix formulation as:

$$\begin{aligned} J^* &= \min_{\delta \delta \underline{f}} \sum_{k=1}^{N_p} \mathbf{E}[\delta \bar{x}_p(k)' Q_0 \delta \bar{x}_p(k)] \\ &+ \sum_{k=0}^{N_p-1} \mathbf{E}[\delta \delta \underline{f}_p(k)' \delta R \delta \delta \underline{f}_p(k)] \end{aligned} \quad (19)$$

where:

- $\delta \bar{x}_p$  and  $\delta \delta \underline{f}_p$  are vectors whose components are the ordered sequence of vectors  $\delta \bar{x}_{i,p}$  and  $\delta \delta f_{i,p}$ ,  $i = 1, \dots, M$ , in a specified time interval  $[t_p, t_{p+1})$ ;
- $Q_0 = \begin{bmatrix} Q_{0,xx} & 0_{3M,M} \\ 0_{M,3M} & \delta R \end{bmatrix} \in \mathbb{R}^{4M}$  is a symmetric positive definite matrix, i.e. the state/control cost matrix, where  $0_{M,N}$  is a matrix of zeros with dimension  $M \times N$ .
- $Q_{0,xx} = \begin{bmatrix} Q_{0,x1} & 0_{M,M} & 0_{M,M} \\ 0_{M,M} & Q_{0,x2} & 0_{M,M} \\ 0_{M,M} & 0_{M,M} & Q_{0,ff} \end{bmatrix} \in \mathbb{R}^{3M}$  is a symmetric positive definite matrix, i.e. the state cost matrix including the control cost at the previous instant, where  $Q_{0,x1} = \text{diag}(p_i)$ ,  $Q_{0,x2} = \text{diag}(h_i)$ , and  $Q_{0,ff} = \text{diag}(r_i)$ .
- $\delta R \in \mathbb{R}^M$  is a diagonal matrix, i.e. the cost function of the control, minimizing the acceleration changes.

For each train, the system evolves according to the linear dynamics given by (18) and it is subject to the stochastic constraints (12), (13), and (14). In addition, another set of constraints is added to limit the variation of acceleration. Specifically:

$$\begin{aligned} \mathbf{E}[\delta \delta f_{i,p}^2(k)] &\leq \delta \delta f_{i,p}^{\max}(k) \quad i = 1, \dots, M \\ & \quad k = 0, \dots, N_p - 1 \end{aligned} \quad (20)$$

These constraints can be put in a generic matrix formulation as shown in (21).

$$\begin{aligned} \mathbf{E} \left[ \begin{bmatrix} \delta \bar{x}_p(k) \\ \delta \delta \underline{f}_p(k) \end{bmatrix}' Q_{r,p} \begin{bmatrix} \delta \bar{x}_p(k) \\ \delta \delta \underline{f}_p(k) \end{bmatrix} \right] &\leq \gamma_{r,p}(k) \\ r = 1, \dots, R = N_p \times (4M - 1) \end{aligned} \quad (21)$$

where

- $Q_{r,p} \in \mathbb{R}^{4M}$  are matrices associated with each constraint given by (12), (13), (14), and (20)
- $\gamma_{r,p}(k) \in \mathbb{R}^{4M-1,1}$  correspond to the right-hand side of constraints (12), (13), (14), and (20), specifically, for the  $k$ -th sample time the following assignments have been given:
  - $\gamma_{r,p}(k) = \underline{x}_{r,p}^{\max}(k)$  in (12)  $r = 1, \dots, M$
  - $\gamma_{r,p}(k) = f_{r,p}^{\max}(k)$  in (13)  $r = M+1, \dots, 2M$

- $\gamma_{r,p}(k) = \delta\delta f_{r,p}^{\max}(k)$  in (20)  $r = 2M + 1, \dots, 3M$
- $\gamma_{r,p}(k) = d_{r,p}^{\max}(k)$  in (14)  $r = 3M + 1, \dots, 4M - 1$

So,  $P^N$  can be resumed according to a more formal and compact notation, as reported hereinafter.

#### Problem $\mathcal{P}_p$

Consider a train platoon subject to the dynamics given for each train by (18), linearized around a planned working state and control at instant  $t_p$ . The problem  $\mathcal{P}_p$  is to find the closed loop optimal control  $\delta\delta f_{-p}(k)$  function of the state as shown in (22)

$$\delta\delta f_{-p}(k) = \mu(\delta\bar{x}_{-p}(k)) \quad k = 0, \dots, N_p - 1 \quad (22)$$

that minimizes the cost function (19), subject to constraints (21), on the time horizon  $[t_p, t_{p+1})$  discretized into  $N_p$  uniform time intervals.

## IV. STOCHASTIC LINEAR QUADRATIC OPTIMAL CONTROL

The problem  $\mathcal{P}_p$  can be solved by the approach for stochastic linear quadratic control [8], resulting in a linear control law. Its main characteristics, with reference to this case study, are summarized by the following theorem.

*theorem* In the problem  $\mathcal{P}_p$ , the optimal control is linear, that is  $\delta\delta f_{-p}(k) = -L_p(k)\delta\bar{x}_{-p}(k)$ , where  $L_p(k)$  is such that:

$$\begin{aligned} & (\bar{B}'S_p(k+1)\bar{B} + Q_{ff}(k))L_p(k) \\ & = \bar{B}'S_p(k+1)\bar{A}_p + Q'_{xf}(k) \\ & k = 0, \dots, N_p - 1 \end{aligned} \quad (23)$$

where  $S_p(N_p) = 0$ , and  $Q_{ff}$ ,  $Q'_{xf}$ ,  $S_p(k+1)$  are defined by the following sequence of problems  $k = 0, \dots, N_p - 1$ :

$$S_p(k) = \max_{\tau_{r,p}(k) \geq 0} \text{Tr} S_p(k) - \sum_{r=1}^R \tau_{r,p}(k) \gamma_p(k) \quad (24)$$

subject to the following linear matrix inequality:

$$Q(k) + \begin{bmatrix} \bar{A}'_p S_p(k+1) \bar{A}_p - S_p(k) & \bar{A}'_p S_p(k+1) \bar{B} \\ \bar{B}' S_p(k+1) \bar{A}_p & \bar{B}' S_p(k+1) \bar{B} \end{bmatrix} \geq 0 \quad (25)$$

$$Q(k) = Q_0 + \sum_{r=1}^R \tau_{r,p}(k) Q_r = \begin{bmatrix} Q_{xx}(k) & Q_{xf}(k) \\ Q'_{xf}(k) & Q_{ff}(k) \end{bmatrix} \quad (26)$$

*Proof:* The demonstration and the specification on the iterative procedure to solve this problem are in [8].  $\square$

#### Note on the theorem

The above theorem considers a perfect observation of the state. Errors in the observation of the state (e.g. GPS measures) are supposed negligible in relation to other potential sources of error. However, it is worth remarking that where there are other sizable measurement disturbances, it can be shown that the related output feedback problem becomes equivalent to state feedback problems  $\mathcal{P}_p$  with a proper application of Kalman filter.

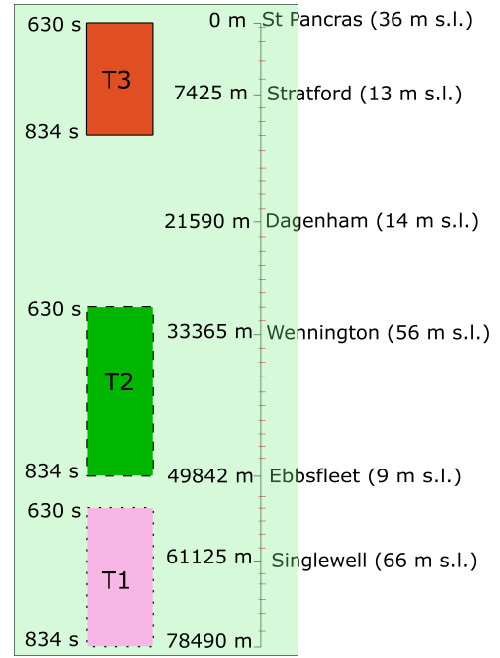


Fig. 5. Track topography on which validation has been achieved. In the time interval 630 - 834 s the three trains T1,T2,T3 are planned to cover a space shown by the related rectangles.

## V. CASE STUDY

The case study refers to the timetable of nine trains over a section of the high-speed Paris-London line. Fig. 5 shows the track topography on which validation has been achieved. Due to the low altitude of each station and the long distance between two consecutive stations, the grade of the track taken into account in (1) is negligible. These trains are scheduled along a single-track line over a period of about three hours, as shown in the timetable presented in Table I. All trains start from the same position (identified by the progressive length, starting from 0, St. Pancras). The length of the single-track line is about 78 km. Two trains (Train 2, Train 6) stop after 31 km approximately (Singlewell).

It can be observed that several platoons form in the network at different time intervals. These platoons are characterized by different numbers of trains. This is evident in Table II showing the trains present in the rail sector in different time periods, according to the scheduled timetable. As instance, in period 2 a platoon of  $M=2$  trains is present, whereas in period 3 a platoon of  $M=3$  trains is formed. Different computations using the proposed approach are therefore required for each time period. Hereinafter, the period number  $p = 3$  is chosen for the application of the proposed approach. As already noted, in this case  $M=3$  and trains 1, 2 and 3 are travelling on the track line. In Fig. 6, the space-time graphs of the selected trains are shown.

The case study has been applied on a time window which lasts 204 s. Specifically, in Fig. 6, the light grey area represents the studied time window: train 3 starts its travel at  $t = 630$  s, train 2 concludes its travel at  $t = 834$  s, while train 1 is covering the selected track line during the interval  $t = 630$  s and  $t = 834$  s.

TABLE I  
TIMETABLE FOR THE 9 TRAINS OF THE CASE STUDY.  
ALL TRAINS ENTER AT POSITION 0

Train sequence number	Enter time [s]	Arrival time [s]	Arrival position [m]
1	0	1410	78490
2	240	834	31690
3	630	2426	78490
4	1440	2850	78490
5	3600	5010	78490
6	3689	4414	31690
7	4230	6026	78490
8	5640	7050	78490
9	7380	8790	78490

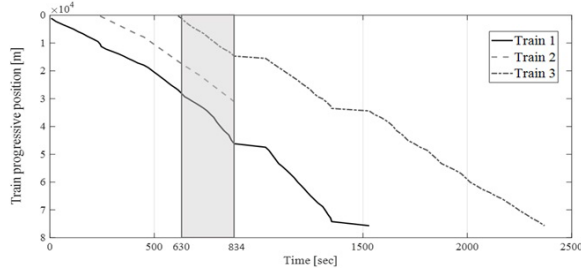


Fig. 6. Progression of the selected trains on the rail line over time.

TABLE II  
PRESENCE OF THE 9 TRAINS OVER THE RAILWAY SECTION

Period $p$	Period Start [s]	Period End [s]	Train numbers															
			1	2	3	4	5	6	7	8	9							
1	0	240	■															
2	240	630		■														
3	630	834			■													
4	834	1410				■												
5	1410	1440					■											
6	1440	2426						■										
7	2426	2850							■									
8	2850	3600								■								
9	3600	3689									■							
10	3689	4230										■						
11	4230	4414											■					
12	4414	5010												■				
13	5010	5640													■			
14	5640	6026														■		
15	6026	7050															■	
16	7050	7380																■
17	7380	8790																■

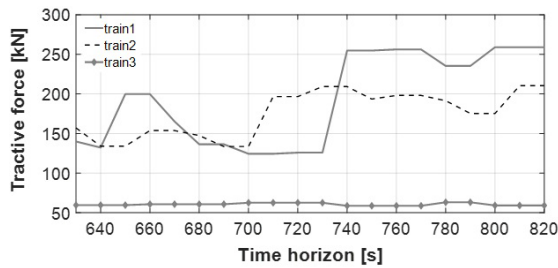


Fig. 7. Planned tractive efforts of the trains in the selected time window.

#### A. Computation of the Control Law

The trains have the same physical characteristics as reported in Table III. The noises contained in matrix  $\bar{W}_p(k)$  are

TABLE III  
PARAMETERS USED IN THE  $P^N$  FOR 3 TRAINS OF THE  
CASE STUDY (PERIOD  $p = 3$  IN TABLE II)

Train Parameter	$W'_i$	$W_i$	$C_i^a$	$C_i^b$	$C_i^c$	$p_i$	$h_i$	$r_i$	$e_i$	$F_{max}$
Values	160	20	9.155	0.06	0.023	10	0.1	1	0.5	360

TABLE IV  
INITIAL RELATIVE POSITION AND SPEED (PERIOD  $p = 3$  IN TABLE II)

Parameter	Train sequence number		
	1	2	3
$\delta \underline{x}_{i,p}(1,0)$	-110	-340	200
$\delta \underline{x}_{i,p}(2,0)$	2	-2	3

TABLE V  
PARAMETER VALUES USED IN THE THREE SCENARIOS

	Scenario I OBJ1	Scenario II OBJ2	Scenario III Tradeoff
$\gamma_{1,p}$	10	1000	500
$\gamma_{2,p}$	10	1000	500
$\gamma_{3,p}$	10	1000	500
$\gamma_{4,p}$	10000	10000	10000
$\gamma_{5,p}$	10000	10000	10000
$\gamma_{6,p}$	10000	10000	10000
$\gamma_{7,p}$	10000	5	10
$\gamma_{8,p}$	10000	100	100
$\gamma_{9,p}$	10000	5	10
$\gamma_{10,p}$	10000	20	100
$\gamma_{11,p}$	10000	20	100

characterized by a Normal distribution  $N(0, 1)$ . The sample time duration is  $\Delta t = 0.1$  s.

In Table IV, the values  $\delta \underline{x}_{i,p}(1, 0)$  and  $\delta \underline{x}_{i,p}(2, 0)$  are respectively the divergence of the initial positions and speeds of the 3 trains with respect to the planned ones.

As regards the matrices and parameters required by the  $R$  constraints defined by (21), they have been set according to three different scenarios, in which some of such constraints have been relaxed. Specifically, the  $\gamma_{r,p}(k)$  are constant in time, that is  $\gamma_{r,p}(k) = \gamma_r$ , and their value in the three scenarios is shown in Table V.

In the first scenario (OBJ1), more relevance is given to track the reference trajectory for each train. So the values  $\gamma_{i,p}$  for  $i = 1, 2, 3$  are relatively low, while the other thresholds are relaxed.

In the second scenario (OBJ2), the parameters have been set to emphasize the minimization of difference between the real and planned positions for two consecutive trains, while also limiting the variation of acceleration.

The third scenario (trade-off) is constrained with lower thresholds with respect to the previous ones. Values of the parameters are defined to obtain a certain trade-off between OBJ1 and OBJ2 scenarios. Table V contains the values of input parameters used in the different simulations.

## VI. RESULTS

The optimal control law has been computed for each train with a receding horizon approach for a time horizon of  $T = 204$  s. For the proposed simulations, a comparison between the planned and actual values for the states and controls variables



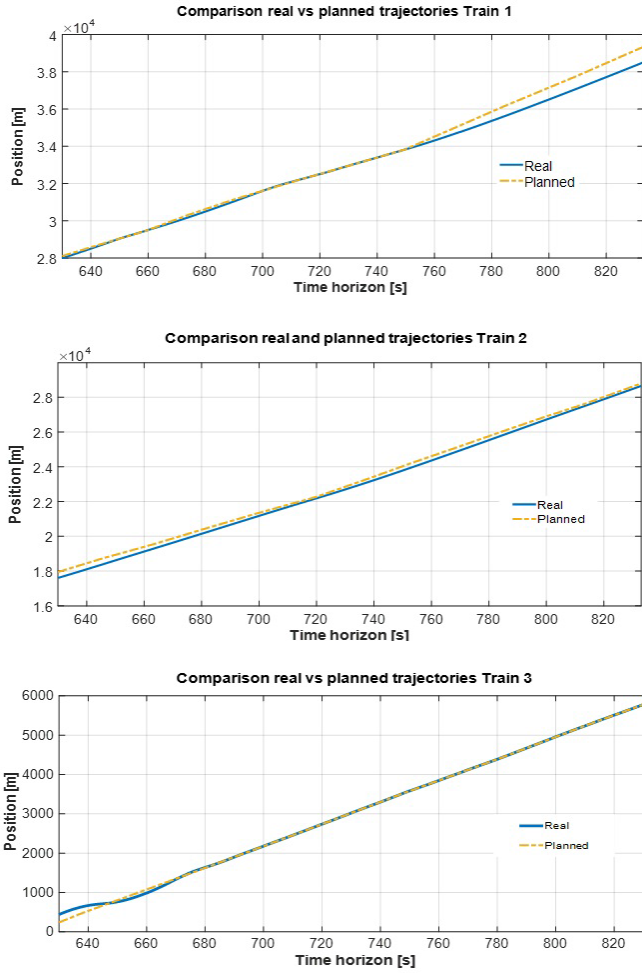


Fig. 8. Trend for the optimal value of the states for the 3 trains for  $T=203$ . (Scenario I) The full lines display the real trajectories while dashed lines represent the planned ones.

have been carried out. In the scenarios, actual tractive effort  $f_i$  of the 3 trains must be limited by the following thresholds [19]:

$$f_i(k) < \min \left\{ \frac{P_{max}}{x_{i,2}(k)}, F_{max} \right\} \quad (27)$$

where  $P_{max}$  and  $F_{max}$  are respectively the current maximum train power and the maximum allowed tractive force, and  $x_{i,2}(k)$  is the actual speed of the  $i$ -th train, at instant  $k$ .

#### A. Scenario I–Tracking Position (OBJ1)

In OBJ1 scenario, the control law generates the best values for the tractive forces to track the desired trajectory for the three different trains.

Fig. 8 shows the optimal positions of the trains with respect to the planned/scheduled ones on a finite horizon of  $t = 204$  s. The figures show a significant tracking of the planned positions more evident for trains 2 and 3 which differ from the planned trajectories respectively for 298 m and 2 m at maximum. However, in the worst case, for train 1, at the end of the time horizon, the real trajectory only diverges for 800 m. This is mainly due to the fact the planned trajectory is hardly feasible for the type of trains used in the case study.

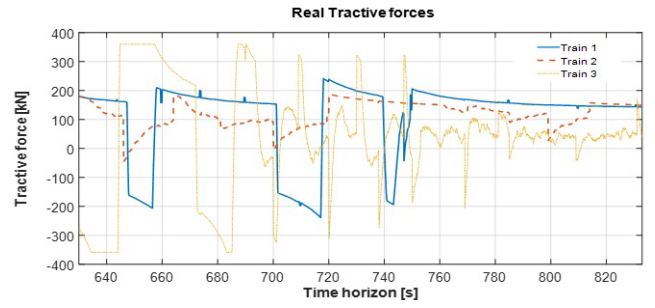


Fig. 9. Trend for the tractive effort for the three trains (scenario I).

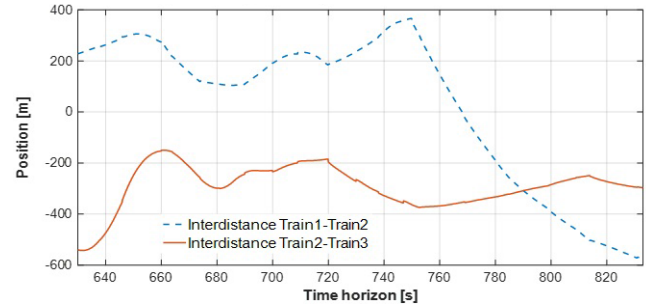


Fig. 10. Divergence of the headway between two consecutive trains in respect to the planned positions (scenario I).

Fig. 9 displays the control variables associated to the tractive forces generated by the trains to carry out their path. It is shown that the constraint (27) related to the maximum allowed value for the tractive effort is respected ( $F_{max} = 360$  kN). Finally, in the Fig. 10, the divergence from the planned headway between two consecutive trains is shown. The lower performances are due to the choice of the parameters  $\gamma_{10}$  and  $\gamma_{11}$  relaxing the constraints related to the position of the train in respect to the previous one.

In quantitative values, the first term of objective (19) has a value of 1102, while the second one reaches 33.

#### B. Scenario II–Limiting Headway Values for Two Consecutive Trains (OBJ2)

In this second scenario, the performances related to the capability of the proposed approach to respect a predefined headway among trains have been tested. In particular, the parameters  $\gamma_r$  assumed the values shown in the second column of Table V. Fig. 11 shows a better performance on the headway with respect to the previous scenario (Fig. 10).

On the other hand, as expected, the tracking of the position (Fig. 12) gets worse for the three trains which, at the end of the time horizon, diverge for about 1000 m from their ideal positions (1030 m for Train 1, 1009 m for Train 2 and 982 m for Train 3).

In quantitative values, the first term of objective (19) has a value of 1442, while the second one reaches 4. As expected the terms related the tractive effort have a lower value than the previous scenario, as the right hand part of the constraints defined by  $\gamma_{7,p}, \gamma_{8,p}, \gamma_{9,p}$  are more restrictive.

Fig. 13 shows the related tractive efforts which are smoother with respect to the ones given by scenario I.

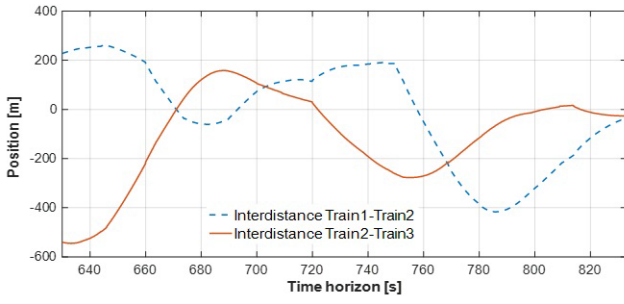


Fig. 11. Divergence of the headway between two consecutive trains in respect to the planned positions (scenario II).

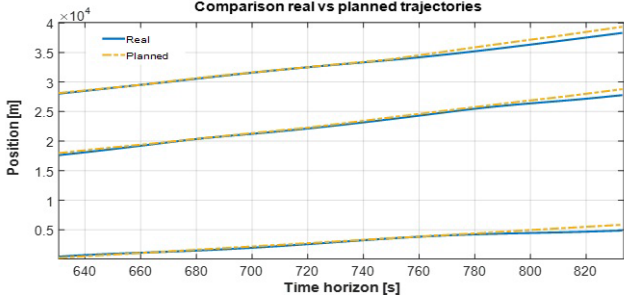


Fig. 12. Trend for the real and planned values of the states for the three trains (scenario II). The full lines display the real trajectories while dashed lines represent the planned ones.

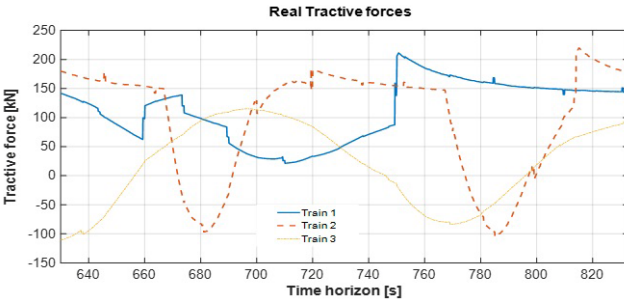


Fig. 13. Tractive efforts of the trains in the scenario II.

### C. Scenario III–Tradeoff Between OBJ1 and OBJ2

The third scenario provides a more constrained scenario where the OBJ1 and OBJ2 are balanced. In this case, the three trains converge to the planned trajectories with a deviation respectively of 970 m, 676 m, and 479 m (Fig. 14). According to the imposed parameter values the divergence for the headways is also reduced compared with the scenario I. In this case, the differences related to the real and planned headways (Fig. 15) are, respectively, about 400 m between Train 1 and Train 2, and 200 m between Train 2 and Train 3. In quantitative values, the first term of objective (19) has a value of 820, while the second one reaches 3. As also shown by the graphs, this scenario represents a good trade-off between the previous ones also in the quantitative values of the relative objective.

Fig. 16 displays the values associated to the actual tractive forces in scenario III.

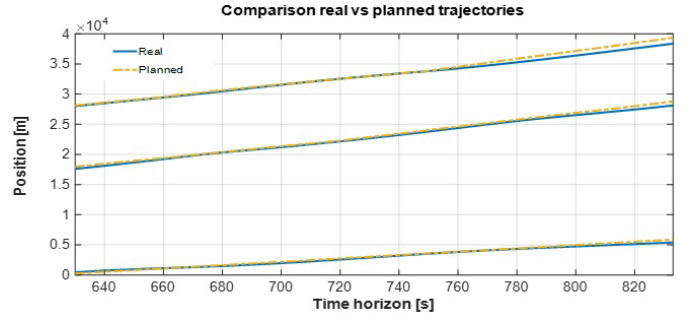


Fig. 14. Trend for the real and planned values of the states for the three trains (scenario III). The full lines display the real trajectories while dashed lines represent the planned ones.

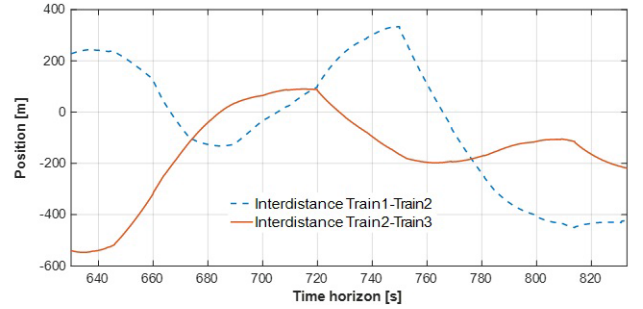


Fig. 15. Divergence of the headway between two consecutive trains in respect to the planned positions (scenario III).

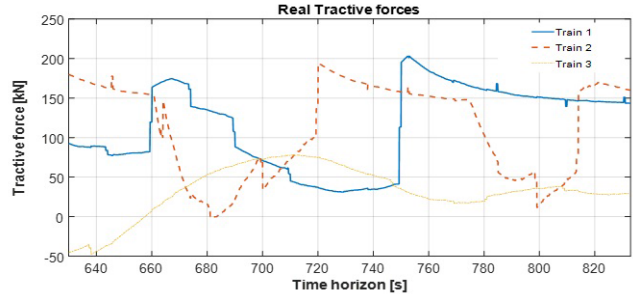


Fig. 16. Tractive efforts of the trains in the scenario III.

## VII. CONCLUSION

Recent research, e.g [20], [21], aims at contributing to the introduction of specific operating modes in the ERTMS/ETCS standard to push railway infrastructure network capacity to its limits in high traffic corridors, while enhancing safety aspects related to the headway control in a train platoon. This work is partially in line with these works, as it aims to contribute to minimize the deviation from pre-planned train schedules which in turn have been designed to optimise the infrastructure capacity, while respecting safety constraints as affected by stochastic noise. Specifically, this work adopts a linear quadratic optimal control problem with stochastic constraints for managing the movement of consecutive trains sharing a single-track railway. In the proposed model, given the position and speed of a train at each time interval, the movements of the trains are modelled by Lomonosoff's equation.

The proposed control model provides the train traffic operators with a methodology which can adjust train timetable deviations suggesting trains' tractive efforts under safe condi-

tions, which is when the headway does not become a critical issue. The introduction of a smoothness penalty of the inputs has been introduced in the control model to reduce sudden variations of the tractive effort.

From a methodological viewpoint, it is worthwhile to underline the innovation introduced by the control strategy that has been applied. Although linear quadratic control approaches, even in a stochastic formulation, are a classic example of the control literature, in this paper, a more recent and innovative generalised formulation proposed by Gattami [8] has been adopted, where the main novelty is the possibility to add quadratic stochastic constraints to the problem formulation, so, limiting the stochastic effects of disturbances on the system. Specifically, the most relevant originality of the paper deals with the possibility to introduce stochastic constraints in a linear quadratic regulator, considering the whole platoon as a system. In fact, the proposed model could be improved under different aspects. For example, the approach could be enhanced taking into account the different dynamic behaviour of tractive and braking forces in the control of the train speed, also considering additional aspects such as energy saving [22]. While in the proposed control model the stochastic constraints are the same both for tractive and braking forces, a more complex behaviour due to perturbed situation can affect braking performances, as shown in previous works [23], [24]. In this context, a future development could be the definition of a switching control approach allowing the combination of different algorithms as recently proposed in a more traditional PID control context [25], applying braking constraints in deceleration contexts and tractive constraints in acceleration ones.

We would expect the method employed to be generalizable to trains that are not physically in a platoon on a single track line, via the concept of virtual platooning that was recently introduced for road vehicles [26]. In conclusion, the proposed linear quadratic optimal control scheme may be a tool suitable for implementation in rail traffic control centres in virtue of its good performance and reduced computational times.

## REFERENCES

- [1] (2016). *Commission Regulation (EU) 2016/919 of 27 May 2016 on the Technical Specification for Interoperability Relating to the 'Control-Command and Signalling' Subsystems of the Rail System in the European Union*. [Online]. Available: <http://eur-lex.europa.eu/legal-content/EN/TXT/?uri=uriserv:OJ.L.2016.158.01.0001.01.ENG&toc=OJ.L.2016.158.TOC.Lastaccess07/08/2016>
- [2] (2008). *Directive 2008/57/EC of the EP and of the Council of 17 June 2008 on the Interoperability of the Rail System Within the Community*. [Online]. Available: <http://eur-lex.europa.eu/LexUriServ/LexUriServ.do?uri=OJ.L.2008:191:0001:0045:EN:PDF>
- [3] S. Sabina, F. Poli, and N. Kassabian, "ERTMS/ETCS railway signalling," in *GNSS for Rail Transportation: Challenges and Opportunities*. Springer, 2018, p. 233.
- [4] J. Farooq and J. Soler, "Radio communication for communications-based train control (CBTC): A tutorial and survey," *IEEE Commun. Surveys Tuts.*, vol. 19, no. 3, pp. 1377–1402, 3rd Quart. 2017.
- [5] *IEEE Recommended Practice for Communications-Based Train Control (CBTC) System Design and Functional Allocations*, IEEE Standard 1474.3-2008, 2008, pp. 1–132.
- [6] S. Morar, "Evolution of communication based train control worldwide," in *Proc. IET Prof. Develop. Course Railway Signalling Control Syst. (RSCS)*, 2012, pp. 218–226.
- [7] X. Dai et al., "Dynamic scheduling, operation control and their integration in high-speed railways: A review of recent research," *IEEE Trans. Intell. Transp. Syst.*, vol. 23, no. 9, pp. 13994–14010, Sep. 2022.
- [8] A. Gattami, "Generalized linear quadratic control," *IEEE Trans. Autom. Control*, vol. 55, no. 1, pp. 131–136, Jan. 2010.
- [9] W. Shangquan, R. Luo, H. Song, and J. Sun, "High-speed train platoon dynamic interval optimization based on resilience adjustment strategy," *IEEE Trans. Intell. Transp. Syst.*, vol. 23, no. 5, pp. 4402–4414, May 2022.
- [10] T. Babczyński and J. Magott, "Dependability and safety analysis of ETCS communication for ERTMS level 3 using performance statecharts and analytic estimation," in *Proc. 9th Int. Conf. Dependability Complex Syst. Brunów, Poland: Springer*, 2014, pp. 37–46.
- [11] K. Guan, Z. Zhong, B. Ai, and T. Kurner, "Propagation measurements and analysis for train stations of high-speed railway at 930 MHz," *IEEE Trans. Veh. Technol.*, vol. 63, no. 8, pp. 3499–3516, Oct. 2014.
- [12] A. Mascis, D. Pacciarelli, and M. Pranzo, "Scheduling models for short-term railway traffic optimisation," in *Computer-Aided Systems in Public Transport*. Cham, Switzerland: Springer, 2008, pp. 71–90.
- [13] S. Li, B. de Schutter, L. Yang, and Z. Gao, "Robust model predictive control for train regulation in underground railway transportation," *IEEE Trans. Control Syst. Technol.*, vol. 24, no. 3, pp. 1075–1083, May 2016.
- [14] J. Felez, Y. Kim, and F. Borrelli, "A model predictive control approach for virtual coupling in railways," *IEEE Trans. Intell. Transp. Syst.*, vol. 20, no. 7, pp. 2728–2739, Jul. 2019.
- [15] Y. Cao, Z.-C. Wang, F. Liu, P. Li, and G. Xie, "Bio-inspired speed curve optimization and sliding mode tracking control for subway trains," *IEEE Trans. Veh. Technol.*, vol. 68, no. 7, pp. 6331–6342, Jul. 2019.
- [16] C. Bersani, S. Qiu, R. Sacile, M. Sallak, and W. Schön, "Rapid, robust, distributed evaluation and control of train scheduling on a single line track," *Control Eng. Pract.*, vol. 35, pp. 12–21, Jan. 2015.
- [17] J. Harbering, A. Ranade, M. Schmidt, and O. Sinnen, "Complexity, bounds and dynamic programming algorithms for single track train scheduling," *Ann. Oper. Res.*, vol. 273, nos. 1–2, pp. 479–500, Feb. 2019.
- [18] E. Krnac and B. Djordjević, "A multi-criteria decision-making framework for the evaluation of train control information systems, the case of ERTMS," *Int. J. Inf. Technol. Decis. Making*, vol. 18, no. 1, pp. 209–239, Jan. 2019.
- [19] S. Lu, S. Hillmansen, and C. Roberts, "A power-management strategy for multiple-unit railroad vehicles," *IEEE Trans. Veh. Technol.*, vol. 60, no. 2, pp. 406–420, Feb. 2011.
- [20] C. Di Meo, M. Di Vaio, F. Flammini, R. Nardone, S. Santini, and V. Vittorini, "ERTMS/ETCS virtual coupling: Proof of concept and numerical analysis," *IEEE Trans. Intell. Transp. Syst.*, vol. 21, no. 6, pp. 2545–2556, Jun. 2020.
- [21] T. Rosberg, T. Cavalcanti, B. Thorslund, E. Prytz, and P. Moertl, "Driveability analysis of the European rail transport management system (ERTMS)—A systematic literature review," *J. Rail Transp. Planning Manage.*, vol. 18, Jun. 2021, Art. no. 100240.
- [22] S. Su, T. Tang, and C. Roberts, "A cooperative train control model for energy saving," *IEEE Trans. Intell. Transp. Syst.*, vol. 16, no. 2, pp. 622–631, Apr. 2014.
- [23] L. Pugi, M. Malvezzi, S. Papini, and S. Tesi, "Simulation of braking performance: The AnsaldoBreda EMU V250 application," *Proc. Inst. Mech. Eng., F, J. Rail Rapid Transit*, vol. 229, no. 2, pp. 160–172, Feb. 2015.
- [24] L. Pugi, M. Malvezzi, S. Papini, and G. Vettori, "Design and preliminary validation of a tool for the simulation of train braking performance," *J. Mod. Transp.*, vol. 21, no. 4, pp. 247–257, Dec. 2013.
- [25] J. Yang, L. Jia, Y. Fu, and S. Lu, "Speed tracking based energy-efficient freight train control through multi-algorithms combination," *IEEE Intell. Transp. Syst. Mag.*, vol. 9, no. 2, pp. 76–90, 2017.
- [26] A. Medina, N. van de Wouw, and H. Nijmeijer, "Cooperative intersection control based on virtual platooning," *IEEE Trans. Intell. Transp. Syst.*, vol. 19, no. 6, pp. 1727–1740, Jun. 2017.

**Chiara Bersani** received the Ph.D. degree in service science applied to transport and logistics systems from the University of Genoa, Italy. She has been a Research Assistant with the University of Genoa since 2007. Her research interests include transport and logistics systems, with special reference to hazardous material management and inventory routing problems.

**Matteo Cardano** is currently pursuing the master's degree in computer engineering with the University of Genoa. He has recently received a Research Fellowship to work in control and systems technologies applied to transportation and logistics.

**Stefano Lavaggi** is currently pursuing the master's degree in computer engineering with the University of Genoa. He has recently received a Research Fellowship assigned to the most talented computer engineering students at the University of Genoa.

**Roberto Sacile** (Member, IEEE) received the master's degree in electronic engineering from the University of Genoa, Italy, in 1990, and the Ph.D. degree in 1994. He has been with the University of Genoa since 2000, where he is currently a Researcher and a Professor of automation and systems engineering. More recently, he has been working in human-machine interfaces to enhance safety in the automotive sector. His research interests include systems engineering and its application to the transportation, logistics, and energy sectors.

**Simona Sacone** (Member, IEEE) received the master's degree in electronic engineering and the Ph.D. degree in electronic engineering and computer science from the University of Genoa, Italy, in 1992 and 1997, respectively. She is currently an Associate Professor of automatic control with the Department of Informatics, Bioengineering, Robotics and Systems Engineering, University of Genoa, where she acts as a Coordinator of the Ph.D. course on systems engineering. She has authored or coauthored more than 150 papers published in international journals, international books, and international conference proceedings. She is the Chair of the Technical Committee on Planning and Control of Transportation Networks of the IEEE Intelligent Transportation Systems Society. She serves as an Associate Editor for the IEEE TRANSACTIONS ON INTELLIGENT TRANSPORTATION SYSTEMS and the *IEEE Control Systems Magazine*.

**Mohamed Sallak** received the Ph.D. degree in dependability assessment of safety instrumented systems under uncertainty from the Polytechnic Institute of Lorraine, Lorraine, France, in 2007, and the Accreditation to Supervise Research (HDR) degree in 2015. He has been an Associate Professor with the Department of Computer Engineering, Université de Technologie de Compiègne, Compiègne, France, since 2009. His current research interests include the reliability assessment of complex systems under uncertainties using several uncertainty theories (belief function theory, imprecise probability theory, and fuzzy set theory), reliability allocation methods, component importance measures, and the dependability assessment of railway systems.

**Enrico Zero** (Member, IEEE) received the master's degree in biostatistics and statistical experimental from the University of Milano-Bicocca in 2015. He is currently pursuing the Ph.D. degree in computer science and system engineering with the University of Genoa. He has been a Research Assistant with the University of Genoa since 2015. His research interests include interactions of automotive data and physiological signals during the road transport of dangerous goods.